UNEC Journal of Engineering and Applied Sciences
Vol. 5, No.1, 2025, pp. 63-69
DOI: https://doi.org/10.61640/ujeas.2025.0507

SECTION: PHYSICAL SCIENCES

Limiting characteristics of silicon diode temperature sensors for determining the maximum temperature with specified measurement accuracy

D.B. Istamov*, O.A. Abdulkhayev, Sh.M. Kuliyev

Physical-technical institute, Academy of Sciences of Uzbekistan, 2B Chingiz Aytmatov str., Tashkent 100084, Uzbekistan
email: *istamov@uzsci.net*

Abstract

This work proposes criteria for establishing a set of electrophysical and structural parameters for silicon-based diode temperature sensors that maximize the sensors' operating temperature while maintaining a specified measurement accuracy. We derived equations from these criteria and developed a mapping graph to illustrate the limiting characteristics. The findings indicate that the operating temperatures of diode temperature sensors can be enhanced by optimizing dopant concentrations and operating currents. Through 3D mapping graphs, we analyzed the maximum operating temperatures and measurement errors of diode temperature sensors. The results demonstrate the potential for diode temperature sensors to operate accurately at temperatures exceeding certain thresholds, as well as at lower temperatures with acceptable accuracy.

***Keywords*:** diode temperature sensor, high temperature, silicon, p-n junction, temperature response curve.

PACS numbers: 74.62.−c, 74.25.Bt

Received:	*Revised:*	*Accepted:*	*Published:*
25 March 2025	*15 April 2025*	*15 May 2025*	*26 May 2025*

1. Introduction

In recent years, the growing demand for high-temperature thermal sensors has advanced the production of Distributed Temperature Sensors into a new stage of development [1-8]. A new type of sensor, combined with a microswitch-based specialized assembly device, offers convenience by integrating all components into a single structure [9-13]. This innovative system features a special heater that activates at the point of data acquisition without influencing the external connection conditions. Additionally, the diode temperature sensor (DTS), positioned some distance from the heater, enables the measurement of pressure, humidity, and mass flow by monitoring temperature [9,14-16]. Since these sensors are primarily derived from silicon structures, it is essential to understand the maximum operating range of silicon-based DTSs.

The relevance of this work lies in determining the maximum temperature range of silicon diode temperature sensors when operating at high temperatures, as well as developing the limiting characteristics that define measurement accuracy. The aim of this research is to enhance the performance efficiency of silicon diode thermal sensors and to expand their potential applications in new conditions.

2. Methodology

In this section, we propose criteria for determining the maximum operating temperature and measurement errors of silicon-based DTS when identifying their limiting characteristics.

To achieve this, we use the following model to determine the limiting characteristics of silicon DTS:

$$V = V_k - \frac{nkT}{q} ln \frac{I_S^*}{I} + \frac{nkT}{q} ln\left(1 + \frac{I_S}{I}\right) \tag{1}$$

where V_k is the built-in potential $[V]$, I_S and I_S^* are the saturation currents for reverse and forward connections $[A/cm^2]$, respectively, q is the charge of an electron [C], V is the voltage across the diode ($p-n$ junction) $[V]$, k is Boltzmann's constant $[N \cdot m^2/C^2]$, T is the temperature $[K]$, and, n is the non-ideality coefficient.

The proposed equation 1 consists of three terms, with the second term, $\frac{nkT}{q} ln \frac{I_S^*}{I}$, representing the variation of the saturation current as a function of temperature. Unlike previous studies [1,11,12], we introduce this second term into the existing model. To derive this term, we propose the following expression for I_S^*:

$$I_S^* = I_s exp\left(\frac{qV_k}{nkT}\right) \tag{2}$$

where I_S^* is introduced as a parameter characterizing the variation of the forward saturation current.

By incorporating this modification, as previously highlighted, we reformulate Shockley's equation, introducing a new term into the final equation, resulting in the form given in equation 1. A detailed description of equation 1 can be found in [17,18].

3. Experimental investigation

The validation of the proposed model was performed by comparing the analytically calculated voltage-temperature dependence with the experimental results reported in [19–21]. figures 1 and 2 illustrate this comparison.

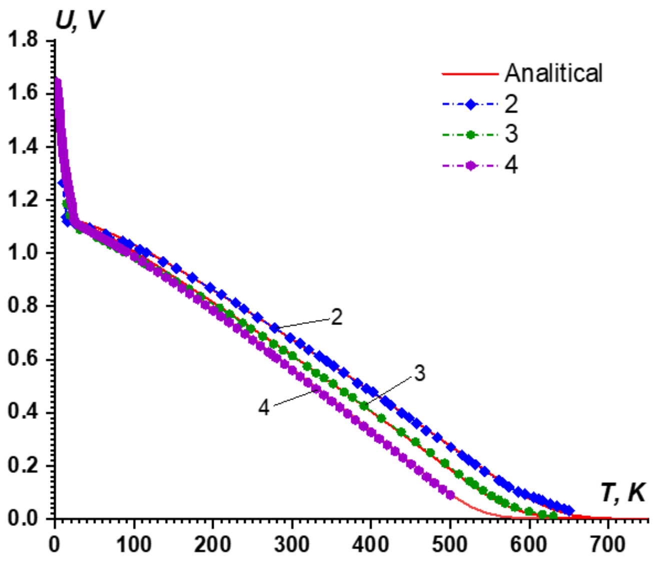

Figure 1. Temperature response curves for silicon diodes: 1 – analytical model (1); experimental data: 2, 3 – [19], 4 – [20]

As observed in figure 1, the analytical calculations closely correspond to the experimental data across almost the entire temperature range. In particular, within the range of $100 < T < 600\,K$, the model exhibits strong agreement with experimental results. However, some deviations are observed at both high and cryogenic temperatures, which may be attributed to experimental conditions, measurement accuracy, and additional physical processes.

In figure 2, discrepancies between the analytical and experimental results can be seen, which may be explained by variations in the current transport mechanism, measurement uncertainties, and systematic errors. Nevertheless, it is important to emphasize that the proposed analytical model is applicable only in cases where the diffusion mechanism dominates the current transport process.

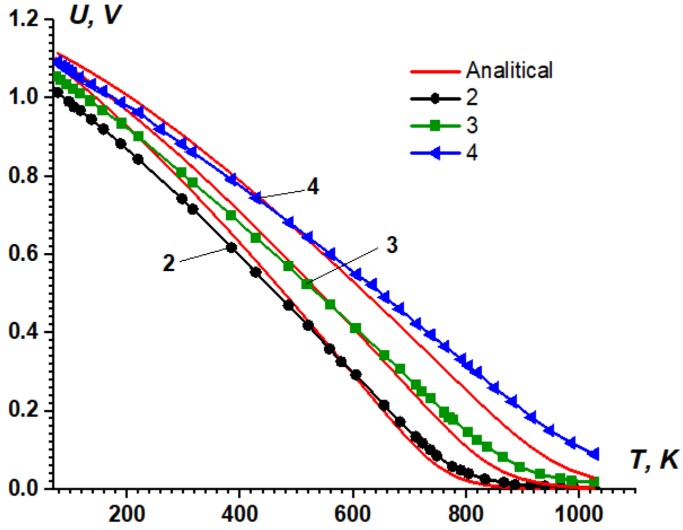

Figure 2. Temperature response curves for silicon diodes: 1– analytical model (1); experimental data: 2,3,4 – [21]

The results presented in figures 1 and 2 were also evaluated statistically. The correlation coefficient (r) and the coefficient of determination (R^2) – which characterize the consistency between the analytical and experimental results – were found to be 0.99 and 0.98, respectively. This confirms the high accuracy of the proposed model.

Furthermore, the error analysis yielded root mean square error (RMSE) and mean absolute error (MAE) values of 0.025 V and 0.02 V, respectively, indicating a strong agreement between the model and experimental data.

Overall, the adequacy of the proposed model for real systems has been validated, suggesting its potential application in future sensor design and optimization processes.

4. Evaluation criteria

Based on this model, we determine the maximum operating temperature and measurement errors of a sensor with a given accuracy using the following criteria:

4.1. Determination of the Maximum Temperature of Silicon Diode Temperature Sensors

The scenarios illustrated in figure 3 include the following:

- Curve 1 represents the complete model graph.

- Curves 2, 3, and 4 correspond to the graphs determined by the first, second, and third terms of equation 1, respectively.

It is well known that temperature sensors operate in a linear region. The point at which the transition to the nonlinear region begins is considered the maximum operating temperature. This transition point occurs when the first and second terms in the model are equal.

From this, by equating the first two terms:

$$V_k = \frac{E_g(T_m)}{q} - \frac{kT_m}{q}\ln\left(\frac{N_V N_C}{N_A N_D}\right) = \frac{nkT_m}{q}\ln\left(\frac{I_S^*}{I}\right) \quad (3)$$

We derive a transcendental equation from expression (2) that enables us to determine the maximum temperature T_m $[K]$:

$$T_m = \frac{E_g(T_m)}{k\ln\left(\frac{N_V N_C}{N_A N_D}\right) + nkln\frac{qS\left(\sqrt{\frac{D_p}{\tau_p}}N_A + \sqrt{\frac{D_n}{\tau_n}}N_D\right)}{I}} \quad (4)$$

where $E_g(T_m)$ is the bandgap energy $[eV]$ at T_m, N_V and N_C are the effective density of states for holes and electrons $[cm^{-3}]$, N_A and N_D are the acceptor and donor concentrations $[cm^{-3}]$, D_p and D_n are the diffusion coefficients for holes and electrons $[cm^2/s]$, τ_p and τ_n are their lifetimes $[ms]$, and S is the heat exchange surface area $[cm^2]$.

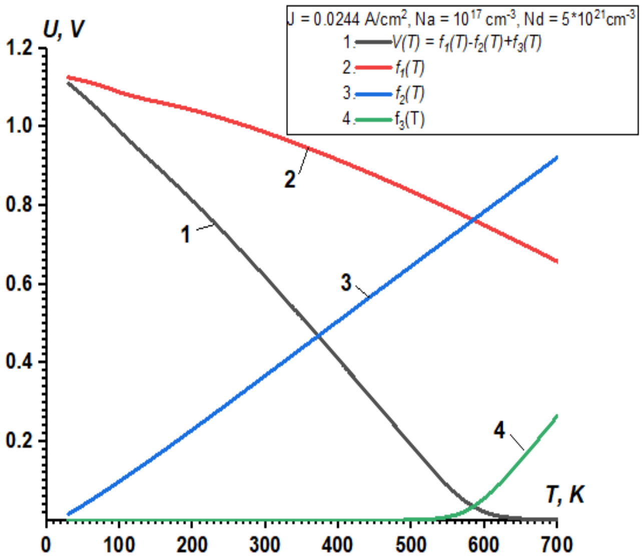

Figure 3. Temperature response curve of Silicon Diodes to temperature sensors

4.2. Systematic errors during diode operation

a) Errors due to self-heating

The current passing through the $p-n$ junction generates Joule heat, leading to self-heating of the diode. Consequently, the temperature of the $p-n$ junction will be higher than the semiconductor surface temperature, which exchanges heat with the environment, by a value of ΔT $[K]$. Therefore, the maximum operating current of the diode is limited by its self-heating process, and the resulting ΔT_H error $[K]$ must not exceed the measurement error ΔT. This is defined as:

$$\Delta T_H = \frac{I \cdot V(I,T)}{S \cdot \lambda_{Si}} l \quad (5)$$

where $P = I \cdot V(I,T)$ is the power dissipated as Joule heat, l is the heat dissipation distance, and, λ_{Si} is the thermal conductivity of silicon $[W/(m \cdot K)]$.

b) Errors due to thermal and shot noise voltages

The minimum operating current of the diode is constrained by the measurement error ΔT caused by the noise voltage U_N across the diode. This is calculated as:

$$\Delta T_N = \frac{U_N}{\alpha(I,T)} = \frac{\left(\frac{2B_W U}{IS}(2kT+qU)\right)^{1/2}}{\alpha(I,T)} \tag{6}$$

where $\alpha(I,T) = \frac{dU}{dT}$ is the thermal sensitivity of the diode, $U_N \equiv \sqrt{\langle U_N{}^2 \rangle}$ is the root mean square noise voltage determined by thermal and shot noise, and B_w is the noise bandwidth.

The error caused by noise voltage is restricted by the minimum current density such that it does not exceed the given ΔT value ($\Delta T_H \leq \Delta T$).

c) Total Systematic Error

The total systematic error of the diode measurement includes the self-heating error and the root mean square noise voltage error, expressed as:

$$\Delta T = \Delta T_H + \Delta T_N \tag{7}$$

This comprehensive approach allows for a clearer understanding of the limitations and operational reliability of silicon diode temperature sensors.

5. Results and discussion

Based on the criteria and equations derived, the mapping graph presented in figure 2 allows for the determination of the limiting characteristics of the sensors. The thermal sensitivity and operating temperature range of temperature sensors primarily depend on the interplay of dopant concentrations in the sensor's base region (N_A,N_D), the operating current (I_d), the temperature (T), and several other parameters. These dependencies are typically evaluated using sensitivity curves, which consider the linear or simple nonlinear relationships among the parameters through conventional analytical methods [1,12,18-20].

In this study, we propose a novel approach to deeply analyze the complex interrelations among these parameters using contour lines and a color scale, as illustrated in figure 4.

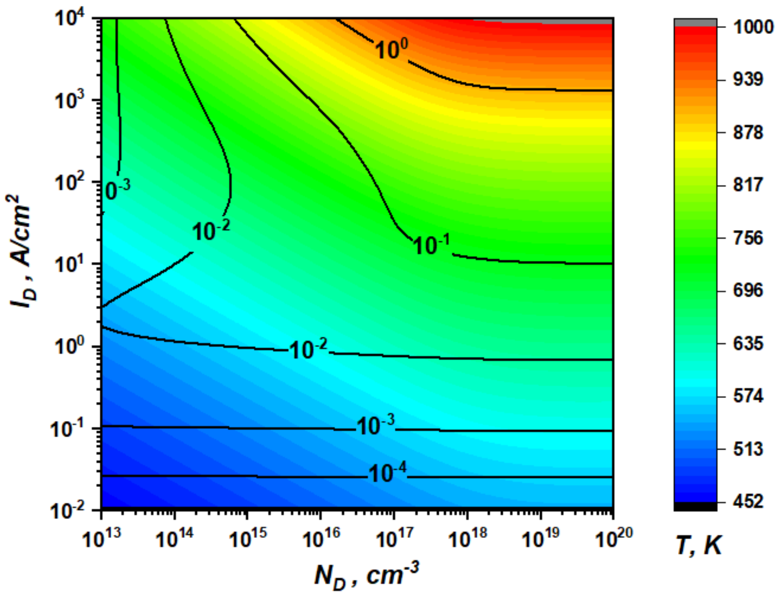

Figure 4. 3D mapping graph representing the limiting characteristics of silicon

This mapping graph visually illustrates the maximum operating temperature of the sensor using a color gradient, while contour lines indicate measurement errors. From figure 4, we can observe the following:

To increase the operating temperature of the DTS, both the dopant concentration and operating current can be maximized, enabling sensors to function at temperatures exceeding $1000\ K$. However, doing so will result in a measurement error of $\Delta T = \pm 10\ K$;

Conversely, for a maximum operating temperature of $750 \div 800\ K$, the sensor can achieve an error of $\pm 0.01\ K$ by increasing the current while using lower dopant concentrations. Alternatively, sensors can be designed for precision by further reducing the dopant concentration, allowing for operation with an accuracy of $\pm 0.001\ K$.

This approach, which identifies the limiting characteristics of silicon diode temperature sensors within specified measurement accuracy, is presented here for the first time. Visualizing these characteristics in a 3D format helps to clarify the intricate relationships and performance metrics involved.

6. Conclusion

This study identified the limiting characteristics that determine the maximum operating temperature and measurement accuracy of silicon diode temperature sensors. The proposed method showed that the sensors' operating ranges could be extended by optimizing factors such as dopant concentrations and operating current. The results indicate that these diode temperature sensors can function at temperatures exceeding 1000 K with a measurement accuracy of ±10 K, or at lower temperatures with an accuracy of ±0.001 K. This significantly enhances the potential applications of these sensors in high-temperature environments, increasing their efficiency and practicality.

Authors' Declaration

The authors declare no conflict of interests regarding the publication of this article.

References

1. M. Mansoor, I. Haneef, S. Akhtar, A. De Luca, and F. Udrea, Sensors and Actuators A: Phys. **232** (2015) 63.
2. S. Rao, G. Pangallo, F. Pezzimenti, and F.G.D. Corte, IEEE Electron Device Lett. **36**(7) (2015) 720.
3. J.Sh. Abdullayev, I.B. Sapaev, East Eur. J. Phys. **3** (2024) 344.
4. S. Santra, F. Udrea, P.K. Guha, S.Z. Ali, and I. Haneef, Microelectronics Journal **41**(9) (2010) 540.
5. R.R. Bebitov, O.A. Abdulkhaev, D.M. Yodgorova, D.B. Istamov, G.M. Khamdamov, Sh.M. Kuliyev, A.A. Khakimov, A.Z. Rakhmatov, Low Temperature Physics **49**(2) (2023) 256.
6. J.Sh. Abdullayev, I.B. Sapaev, Eurasian Physical Technical Journal **21**(3(49)) (2024) 21.
7. J.Sh. Abdullayev, I.B. Sapaev, Physical Sciences and Technology (Phys. sci. technol) **11**(3-4) (2024) 39.
8. R.R. Bebitov, O.A. Abdulkhaev, D.M. Yodgorova, D.B. Istamov, Sh.M. Kuliyev, A.A. Khakimov, A.B. Bobonazarov, A.Z. Rakhmatov, Low Temperature Physics **50**(5) (2024) 458.
9. E.L.W. Gardner, J.W. Gardner, and F. Udrea, Sensors **23**(2) (2023) 681.
10. M. Kimura, Lect. Notes Electr. Eng. **49** (2009) 309.
11. M. Kimura and K. Toshima, Sensors and Actuators, A: Physical **108**(1–3) (2003) 239.
12. A. De Luca, V. Pathirana, S.Z. Ali, D. Dragomirescu, and F. Udrea. Sensors Actuators, A Phys. **222** (2015) 31.

13. P.K. Guha, S.Z. Ali, C.C.C. Lee, F. Udrea, W.I. Milne, T. Iwaki, J.A. Covington, J.W. Gardner, Sensors Actuators, B Chem. **127**(1) (2007) 260.
14. L. Ribeiro, O. Saotome, R. d'Amore, R. de Oliveira Hansen, Sensors **22**(9) (2022) 3484.
15. Y. Zhang and Y. Jiang, IEEE Sensors Journal **23**(6) (2023) 5718.
16. F. Ejeian, Sh. Azadi, A. Razmjou, Y. Orooji, A. Kottapalli, M. Ebrahimi Warkiani, M. Asadnia, Sensors and Actuators: A Phys. **295** (2019) 483.
17. D.B. Istamov, O.A. Abdulxayev, Scientific Bulletin of NamSU **2** (2024) 39.
18. D.B. Istamov, O.A. Abdulkhaev, A.A. Khakimov, K.N. Allakulov, D.M. Yodgorova, A.Z. Rakhmatov, Uzbek Journal of Physics **26**(4) (2025) 1.
19. Y.M. Shwarts, V.L. Borblik, N.R. Kulish, E.F. Venger, and V.N. Sokolov, Sensors and Actuators: A Phys. **86**(3) (2000) 197.
20. S.S. Courts, Cryogenics **74** (2016) 172.
21. A. De Luca, V. Pathirana, S.Z. Ali, D. Dragomirescu, and F. Udrea, Sensors and Actuators: A Phys. **222** (2015) 31.